

STUDIES OF THE MEDIUM-TERM EFFECT OF NANOCONSOLIDANTS ON WALL PAINT LAYERS WITH A LACK OF COHESION

Penka I. GIRGINOVA¹*, Milene GIL¹

¹HERCULES Laboratory and IN2PAST, IIFA, University of Évora, Palácio do Vimioso, Largo Marquês de Marialva, 8, 7000-809 Évora, Portugal.

Abstract

This paper reports an updated overview of a comparative study on the medium-term effects of treatment with three consolidants—laboratory-prepared nanolime, commercial nanolime, and commercial acrylic resin—on fresco paint layers replicas affected by lack of cohesion. This is a follow-up to our preliminary data published in 2021. In 2020, paint layers replicas of frescos were prepared in vitro by buon and lime fresco painting techniques with blue smalt and yellow ochre pigments. The samples were treated with the three consolidants and aged at ambient conditions. In 2023, the authors repeated the analysis to assess and compare the three-year effect of the laboratory-prepared nanolime on the paint layers with regard to the commercial nanolime and acrylic resin. The analytical setup comprised photography, scanning electron microscopy coupled with energy dispersive x-ray spectroscopy, and colorimetry or spectrophotometry. Monitored parameters were the impact of the treatments on the paint layer morphology and on the colour. After three years, the presence of all products is still detected on the paint surface, where they maintain their effects on the paint layer morphology. Aesthetical changes that occurred immediately after the treatment have maintained a relatively constant value over the course of time.

Keywords: Nanolime; Consolidants; Frescoes; Medium-term effect; SEM-EDS

Introduction

Frescoes paintings, as any other artwork, are subject to ageing and deterioration as threatened by natural and human impacts, which over time may severely affect their aesthetic appearance, composition, and structure [1, 2]. Among the deterioration features that are commonly found is the lack of cohesion of the paint layers and mortars caused by the disruptive presence and activity of salts. This kind of decay brings about the need for a consolidation treatment in order to strengthen the crystalline network and improve the mechanical resistance within the layer's structure.

Nanolime has been seen as a very promising alternative to traditional consolidants (e.g., organic and silane-based materials) for the preservation of different decayed substrates, such as fresco wall paintings [3-5], since the pioneering works of Baglioni's group [6]. However, the consolidation treatment with nanolime is rather complex [5, 7-9]. Despite the research already undertaken on the best dispersing solvents, the synthesis methods of the nanolimes applied, and application manners, there is still a lack of a full understanding of how the treatment would affect the paint surfaces over a longer time frame. In particular, there are still doubts raised by

* Corresponding author: penka@uevora.pt

conservator-restorers about the mechanisms of white haze formation and how to avoid white haze formation due to the treatment. In order to avoid any aesthetic changes, different factors must be taken into account in the studies. Among these factors are: i) what is the optimal particle diffusion depth in order to ensure maximal strengthening of the network; ii) how they ensure the consolidation process and a complete carbonation; and iii) how the nature of the pigments, the preparation techniques of the pictorial layers, the origin of the damage, and the degree of deterioration of the substrate will influence this effect. There are several attempts to reduce the veil, for example, by varying the application method and conducting a cleaning treatment [10], but this could be too aggressive for the pictorial layer. The appearance of the white veil might be reduced not only by the control of the nanolime and substrate characteristics but also with the use of, for example, wet cellulose poultices. The application procedure must be chosen with respect to the nanolime morphology and the specific characteristics of the substrate, where the penetration depth of the particles should not be limited [8]. The carbonation and microclimatic conditions, especially the relative humidity, moisture, and salt contents, can hinder the improvement of the cohesion of the paint layers after treatment with nanolime without having an impact on other physical properties [11].

In the course of our studies on fresco wall paintings and on the development of innovative materials for cultural heritage, we have analysed the effectiveness potential of laboratory-synthesised nanolime for the restoration of fresco paintings [12–14]. Preliminary results have been reported in 2021 as an approach to widening the understanding of the effect of two nanolimes (laboratory-synthesised calcium hydroxide nanolime and commercial calcium hydroxide-based nanolime) and traditionally used commercial acrylic-based resin produced on a set of frescoes painted replicas with a lack of cohesion [15]. The study has discussed the *in vitro* assays that were performed before and a short time after treatment (in one week and one month) with the three kinds of consolidants applied by nebulization over two sets of replicas of *buon* and lime frescos painted with red and yellow ochres and smalt pigments [15]. Herein, our recent survey of the paint layers three years after treatment will be discussed. This is a comparative and ongoing study of the medium-term effects of treatment with the three consolidant materials on fresco paint layers affected by a lack of cohesion.

The effect of the consolidants on the surface morphology and the colours of the treated replicas is discussed. With this research, we intend to contribute towards a better understanding of the medium-term effect of the nanolimes on *buon* and lime fresco paint layers that would be beneficial for conservators and restorers.

Experimental part

Materials and methods

The analyses were carried out on fresco paint layers replicas with a lack of cohesion (dimensions 5x5x5cm) prepared *in vitro* and treated with three kinds of consolidants, as described in detail in our previous study [15]. The smalt and yellow ochre replicas analysed in this study were prepared or treated with the same set of samples from the cited previous study; however, the reported analyses were conducted on different samples.

The renderings of the fresco replicas consist of two layers of lime-based mortars. The inner layer of *arriccio* was made from coarser siliceous-based aggregates (1 part of hydrated lime putty and 2 parts of siliceous sand). The superficial layer, *intonaco*, was made from finer calcium-based aggregates (1 part of hydrated lime putty and 2 parts of cream marble). Paint layers replicas were prepared by *buon* fresco (BF) and lime fresco (LF) painting techniques with yellow ochre pigment (y-LF, y-BF) and blue smalt pigment (only prepared in lime fresco, b-LF) (Figure 1a and Table 1).

In both BF and LF techniques, the pigments are fixed by carbonation reaction, but while in *buon* fresco the pigments were mixed only with pure water, for lime fresco the pigments

were dissolved in calcium hydroxide (in this case lime milk). The two kinds of pigments, both widely used with particular historical and artistic significance, were selected due to their different natures, origins, and resistance to weathering conditions [16, 17].

Figure 1a illustrates the selected paint layers and their characteristics: type of pigment used, preparation technique, and applied consolidant. Once the paint layers were prepared, the fresco sets remained to dry for one month in the laboratory under ambient conditions, as reported [15] ($T = 22 \pm 2^\circ\text{C}$, $\text{RH} = 57 \pm 9\%$). Afterward, and for further analysis, the paint surface of each replica was divided into four equal areas (Fig. 1b) [15].

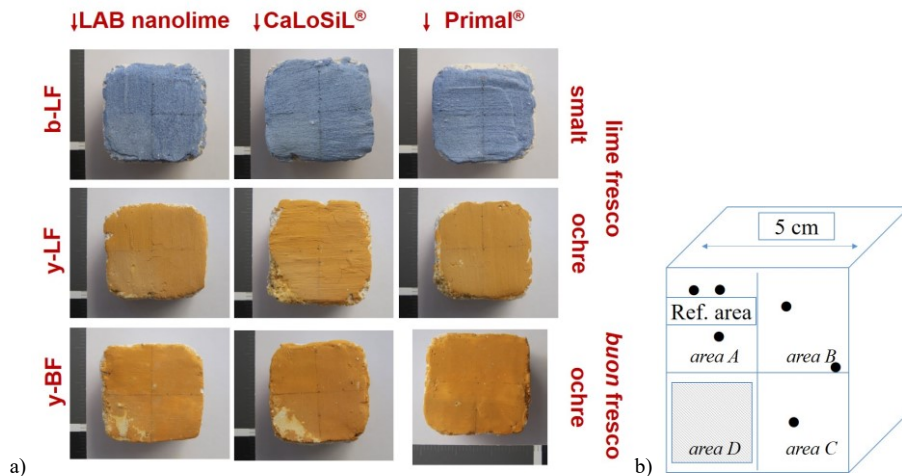


Fig. 1. Replicas representation:

- a) Photographic documentation of the paint layers and their characteristics;
 b) Schematic representation of the surface division:
 area A - untreated, naturally induced lack of cohesion;
 areas B/C - treated, naturally induced lack of cohesion;
 area D: treated, mechanically induced deterioration.
 Analysed points with colorimetry are shown as small dots

Area A was untreated and therefore selected as a reference. Areas B, C and D were afterwards treated (see below). Areas A, B and C presented natural deterioration in their paint surfaces, while we induced mechanically higher degradation in area D by scratching the surface with a sharp tip. In two of the *buon* fresco replicas, the induced abrasion also caused flaking of the paint layers due to the higher pressure applied. After drying, the replicas were treated with three consolidant products (Table 1) by nebulization (area A was kept covered to remain untreated) [15]:

1-laboratory prepared nanolime (LAB nanolime), dispersion of $\text{Ca}(\text{OH})_2$ nanoparticles (size between 18–713nm), 25g/L in Acetone:Ethanol (1:10);

2-CaLoSiL® IP25, dispersion of $\text{Ca}(\text{OH})_2$ nanoparticles (size between 50–250nm, Technical Datasheet), 25g/L in iso-propanol (IBZ Salzchemie GmbH & Co. KG, Halsbruecke, Germany);

3-Primal™ SF-016 ER® Acrylic polymer dispersion (Dow Coating Materials, United States of America): 50–51% solid content; applied diluted at 2% v/v in tap water).

The first set of analyses was carried out just after the treatment in 2020 [15]. In 2023, after three years of natural ageing (at *ca.* 18–30°C and 50–70%RH), the same analytical setup was repeated for comparison. It included photographic documentation in the Visible (Vis), spectrophotometry and colorimetry in the Vis, and scanning electron microscopy with energy dispersive spectroscopy (SEM-EDS).

Table 1. Samples and areas designation; replicas references, composition, preparation technique and treatment.

Sample ref.	Pigment	Preparation technique	Applied consolidant
b-LF-1	blue smalt	lime fresco	LAB nanolime, 25g/L, Ca(OH) ₂ in 2-propanol
b-LF-2	blue smalt	lime fresco	Commercial nanolime, CaLoSiL® IP25 (25g/L, Ca(OH) ₂ -based in 2-propanol
b-LF-3	blue smalt	lime fresco	Commercial acrylic resin, Primal™ SF-016 ER®, 2% v/v
y-LF-1	yellow ochre	lime fresco	LAB nanolime, 25g/L, Ca(OH) ₂ in 2-propanol
y-LF-2	yellow ochre	lime fresco	Commercial nanolime, CaLoSiL® IP25 (25g/L, Ca(OH) ₂ -based in 2-propanol
y-LF-2	yellow ochre	lime fresco	Commercial acrylic resin, Primal™ SF-016 ER®, 2% v/v
y-BF-1	yellow ochre	<i>buon</i> fresco	LAB nanolime, 25 g/L, Ca(OH) ₂ in 2-propanol
y-BF-2	yellow ochre	<i>buon</i> fresco	Commercial nanolime, CaLoSiL® IP25 (25g/L, Ca(OH) ₂ -based in 2-propanol
y-BF-3	yellow ochre	<i>buon</i> fresco	Commercial acrylic resin, Primal™ SF-016 ER®, 2% v/v
Area			
A	Presents naturally induced lack of cohesion of the paint surface. Untreated.		
B/C	Presents naturally induced lack of cohesion of the paint surface. Treated.		
D	Presents mechanically induced deterioration of the paint surface. Treated.		

SEM-EDS provided fundamental insights into the consolidated paint surfaces by allowing us to ascertain the presence of the three consolidants and the comparison between the treated and untreated paint surfaces. The EDS provided information on the elemental distribution and semi-qualitative elemental analysis. Spectrophotometry and colorimetry in the Vis are permitted to monitor the possible colour changes after three years of ageing.

Photographic documentation

The overview photos of the replicas were captured in daylight with a Canon EOS 800D 24Mpx. Raw image output was used with target QpCard101 v3 for white balance calibration.

Scanning electron microscopy-Energy dispersive spectroscopy (SEM-EDS)

SEM-EDS analysis of the replicas has been performed using a Hitachi S-3700N (Hitachi High Technologies, Berlin, Germany) Scanning Electron Microscope coupled with an energy dispersive X-ray spectrometer BRUKER XFlash 5010 SDD EDS. The analysis was performed under variable pressure, operated with accelerating voltages of 20kV in backscattered electron (BSE) mode. EDS analysis and quantification were acquired with Esprit 1.9 software from Brüker corporation.

Colorimetry and spectrophotometry

Colorimetry and spectrophotometry were measured with a Data Color Check Plus II, in SCE and Standard Illuminant/Observer D65/10° and aperture size USAV (Ø 25mm). The colour changes between untreated (area A) and treated areas (B/C) were evaluated by measuring colour variations (ΔE^*), which were calculated according to Equation (1) [18].

$$\Delta E^*_{ab} = [(\Delta L^*)^2 + (\Delta a^*)^2 + (\Delta b^*)^2]^{1/2} \quad (1)$$

ΔL^* , Δa^* , and Δb^* correspond to variations in the colour values in the dark–light, red–green, and yellow–blue axes, respectively. The parameters were calculated according to Equations (2–4), where "sample" is the value measured on treated areas and "standard" is the measured on untreated areas A (Figure 1b).

$$\Delta L^* = L^*(\text{sample}) - L^*(\text{standard}) \quad (2)$$

$$\Delta a^* = a^*(\text{sample}) - a^*(\text{standard}) \quad (3)$$

$$\Delta b^* = b^*(\text{sample}) - b^*(\text{standard}) \quad (4)$$

For each area (A, B/C), the average of 3 measurements (three points and three light flashes) was considered. The average of the three measurements was calculated with standard deviation in consideration.

Results and discussion

Smalt/lime fresco replica treated with LAB nanolime

The SEM-EDS microscopy analysis of untreated and treated with LAB nanolime areas of smalt/lime fresco replica (sample b-LF-1) is shown in figure 2. Area A represents the untreated porous matrix (Fig. 2a). The elemental map distribution of area A confirms the large presence of Ca (calcium) from the carbonated lime binder to calcite (CaCO_3), Si (silicon), mostly from the aggregate (grains of sand), and Co (cobalt) from the smalt pigment. Apart from the calcite surface matrix mixed with the smalt pigment grains, on the treated areas B and D, there are hexagonal plate-like and rectangle-like-shaped particles spread over the surface of the sample (Fig. 2b and c, solid line arrows). The particles are distributed heterogeneously, single and clustered together between and over the grains of the calcite, sand, and pigment, covering the pores of the calcite network. The surface areas covered with particles are enriched in Ca (Fig. 2b and c; EDS points 4, 5). In addition, there are also several spots covered with a thin calcium-based coating layer (Fig. 2b and c, dashed line arrows, EDS points 3, 6), formed over the aggregate grains, providing links between the aggregate and the calcite matrix.

The observed particles share the same morphological characteristics as the $\text{Ca}(\text{OH})_2$ LAB nanolime that was applied [15]. They have been prepared by bottom-up precipitation homogenous reaction in water with a non-ionic surfactant, Triton X-100 (the synthesis and characterization have been described in detail in reference [15]). The hexagonal plate-like nanoparticle shapes and the tendency to agglomerate in clusters are, indeed, characteristics of $\text{Ca}(\text{OH})_2$ nanoparticles obtained by this method [20]. Such hexagonal particle clusters were observed over the paint layers after one week of treatment. Consequently, it is possible to assume that the hexagonal particles observed are uncarbonated LAB nanolime $\text{Ca}(\text{OH})_2$ nanoparticles. The small amount of rectangle-like particles seems to be carbonated single nanolime particles to CaCO_3 polymorphs, carbonated during the nanolime storage [13] or after the applications, similarly to what was already observed after treatment of limestone [19]. These particles were carbonated before bonding with the replica matrix, as they have a smaller size compared to the calcite from the replica paint layer.

These two kinds of particles have remained on the surface, as they were already observed in the preliminary studies one week after treatment [15]. Interestingly, the thin calcium-based coating layer is newly formed compared to the preliminary analyses in 2020, when only the treatment with commercial nanolime led to a layer formation. This kind of Ca-rich layer occurred in the treated samples with the LAB nanolime in three years. The treatment with the commercial nanolime ($\text{CaLoSiL}^{\text{®}}$) led to the formation of such a coating layer with a homogenous appearance on the painted surfaces after one week of treatment, while a similar layer was not observed in one week after treatment with the LAB nanolime, but it appeared on the paint layers in images captured three years after treatment. In the former case, the coating is thinner and covers smaller areas of the replica surface.

Yellow ochre/lime fresco replica treated with LAB nanolime

Identical hexagonal plate-like and rectangle-like nanoparticles clustered together were observed over the paint layer of the yellow ochre lime fresco treated with LAB nanolime (Fig. 3). The particles that did not diffuse in the lime mortar network of the replica and appear heterogeneously accumulated on the paint layers as: a) clustered $\text{Ca}(\text{OH})_2$ nanoparticles; and b) partially carbonated single particles to CaCO_3 rectangle-like polymorphs (solid line arrows).

Also, c) a coating layer appears in spots (dashed line arrows) that are more compact than in the case of the smalt samples (Figs. 2b and c, and 3c). In the elemental distribution maps, the element Si is associated with the aggregate, Ca (with the calcite carbonated from the lime binder) and the applied consolidant, and iron (Fe) with the ochre pigment. In figure 3, middle and bottom images, clusters of nanoparticles can be seen that are of the same morphological appearance as the applied LAB nanolime consolidant [15].

Yellow ochre/buon fresco replica treated with LAB nanolime

LAB nanolime particles remain spread over the ochre *buon* fresco layer in similarity to the case of lime fresco preparation (Fig. 4). The thin carbonated layer appears observable only over spots in area D. Area D is the most deteriorated area where there are fewer pigment grains, therefore there is a more favourable calcite environment to recuperate the substrate network (Fig. 4c).

Smalt and yellow ochre/lime fresco replicas treated with commercial nanolime

The Ca-rich coating layer observed in the medium term, formed by the commercial nanolime onto the replicas of blue and yellow lime frescos, b-LF-2 and y-LF-2 (Figs. 5 and 6), is denser and covers a larger surface area than in the case of the spots formed from the LAB nanolime. These coating layers are rather dense and spread between grains of the aggregate from the *intonaco*, covering the grains of lime binder or calcite mixed with the pigment, which is more evident in the case of the more deteriorated area D of b-LF-2 and more compact and evident on the ochre sample y-LF-2. The two coatings are similar to those formed in 2020, one week after the sample treatment, indicating that they have remained unchanged upon ageing during the next three years, maintaining the re-cohesion of the paint layer and making them as efficient as immediately after the treatment, given that no detachments or cracks are present.

Yellow ochre/buon fresco replica treated with the commercial nanolime

The coating layer formed after the treatment with the commercial nanolime appears less compact over area D of the *buon* fresco sample y-BF-2 (Fig. 7), while area B is covered by denser Ca-rich spherical like spots.

The observations in 2023 and the data comparison with 2020 suggest that LAB nanolime is subject to slower carbonation compared to commercial nanolime. The two consolidants were applied in different solvent formulations: Acetone:Ethanol (the LAB nanolime) and isopropanol (CaLoSiL[®]). Also, the particle diagonals of the LAB particles were measured as between 18–713nm, while the dimensions of the CaLoSiL[®] IP25 particles were between 50–250nm (Technical Datasheet) [15]. The kinetics of carbonation depend on a range of parameters, such as the hydration of CO₂, surface area of the nanolime particles (i.e., particle dimensions), relative humidity, temperature, possible additives, mixture of dispersing solvents applied/possible addition of water to the alcohol, or addition of a carbonate source [3, 7]. These parameters can affect the system's supersaturation, which controls the nucleation density of carbonate phases and their evolution [3]. In agreement with the studies of *C. Rodríguez-Navarro et al.* [3] and *R. Camerini et al.* [21], the CaCO₃ polymorph evolution is ACC-vaterite (aragonite)-calcite [3, 21], where the formation of calcite takes place through either direct (nucleation from solution) or indirect pathways (through nucleation on vaterite and aragonite). Given that it is possible that calcite coexists with vaterite starting from the first stages of the formation of crystalline phases [21] and that the polymorph evolution is slower for larger nanoparticles (with lower surface area) [21], we could expect that the conversion of the LAB nanoparticles Ca(OH)₂ into CaCO₃ would be partial, incomplete, and slower than the conversion of the commercial nanolime nanoparticles.

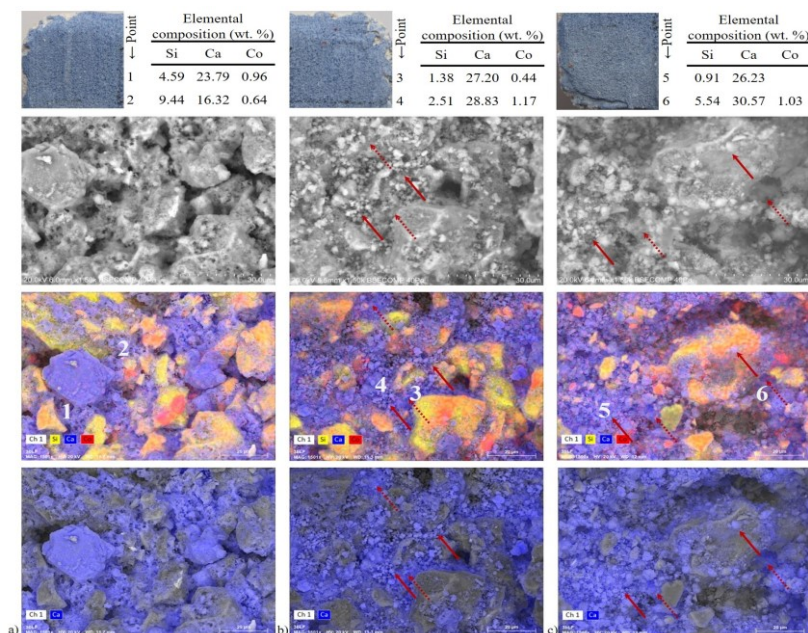


Fig. 2. SEM images (top) and SEM-EDS elemental distribution maps (Si, Ca, Co – middle; Ca – bottom) of sample b-LF-1. a) Area A - untreated; b) Area B (treated with LAB nanolime); c) Area D (treated with LAB nanolime). *Solid line arrows point out hexagonal and rectangles-like shaped particles; dashed line arrows show the thin coating layer formations. (Insets: left - photography capture of the analysed area; right - EDS point analysis: elemental composition, main elements.)*

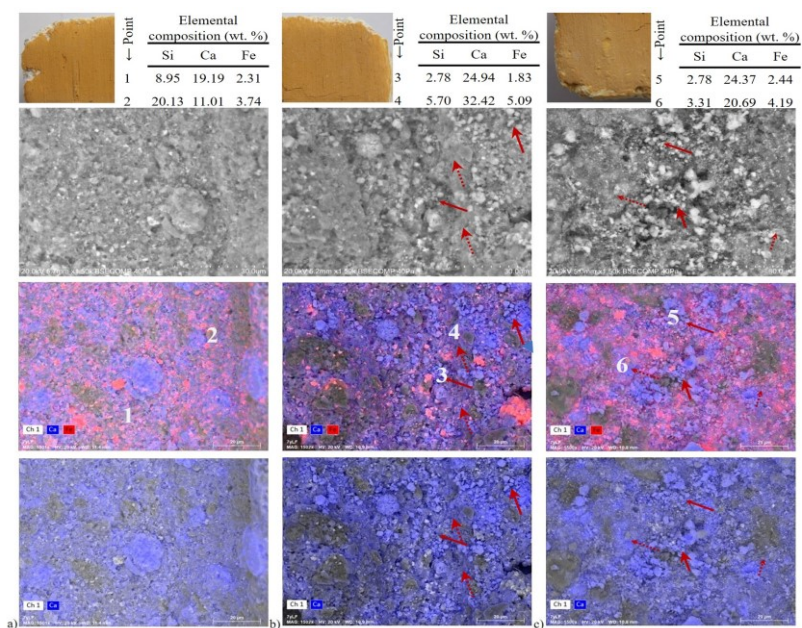


Fig. 3. SEM images (top) and SEM-EDS elemental distribution maps (Ca, Fe – middle; Ca – bottom) of sample y-LF-1. A) Area A – untreated; b) Area B (treated with LAB nanolime); c) Area D (treated with LAB nanolime). *(Insets: technical photography capture of the analysed area.) Solid line arrows point out hexagonal and rectangles-like shaped particles; dashed line arrows show the thin coating layer formations. (Insets: left – photography capture of the analysed area; right – EDS point analysis: elemental composition, main elements)*

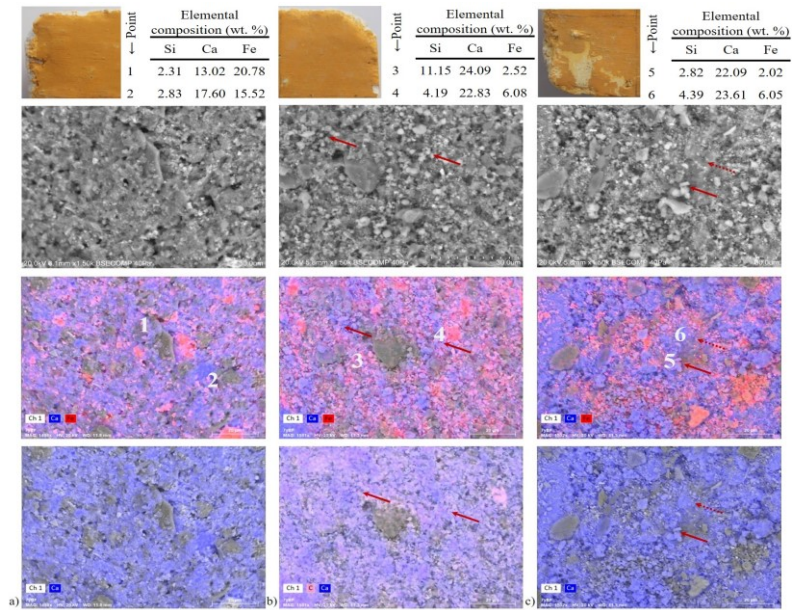


Fig. 4. SEM images (top) and SEM-EDS elemental distribution maps (Ca, Fe – middle; Ca - bottom) of sample y-BF-1. a) Area A - untreated; b) Area B; c) Area D. (Insets: technical photography capture of the analysed area.). Solid line arrows point out single-like crystals of the nanoparticles (nanolime and carbonated particles); dashed line arrows show the thin coating layer formations.

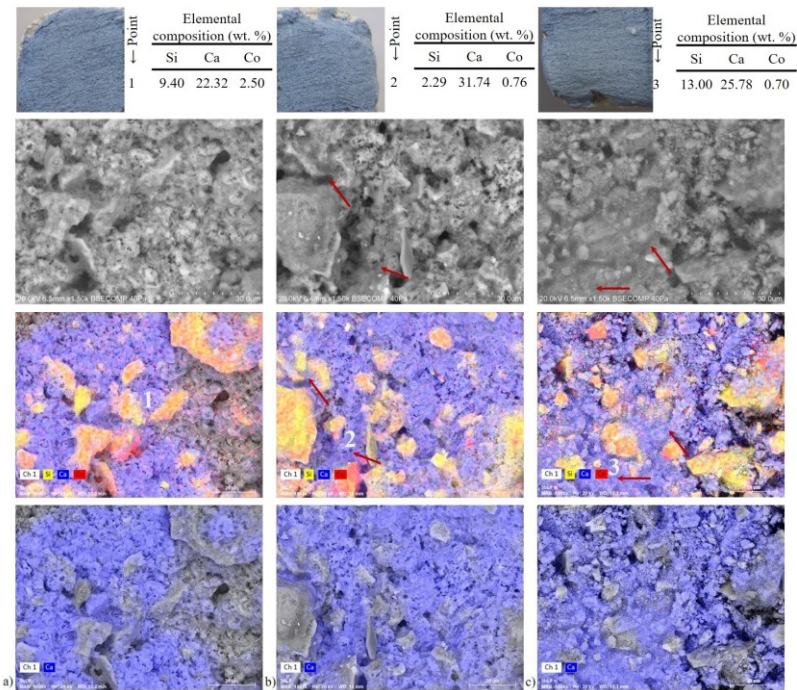


Fig. 5. SEM images (top) and SEM-EDS elemental distribution maps (Si, Ca, Co – middle; Ca – bottom) of sample b-LF-2. a) Area A - untreated; b) Area B; c) Area D. (Insets: technical photography capture of the analysed area.) Solid line arrows point out the coating layer formed

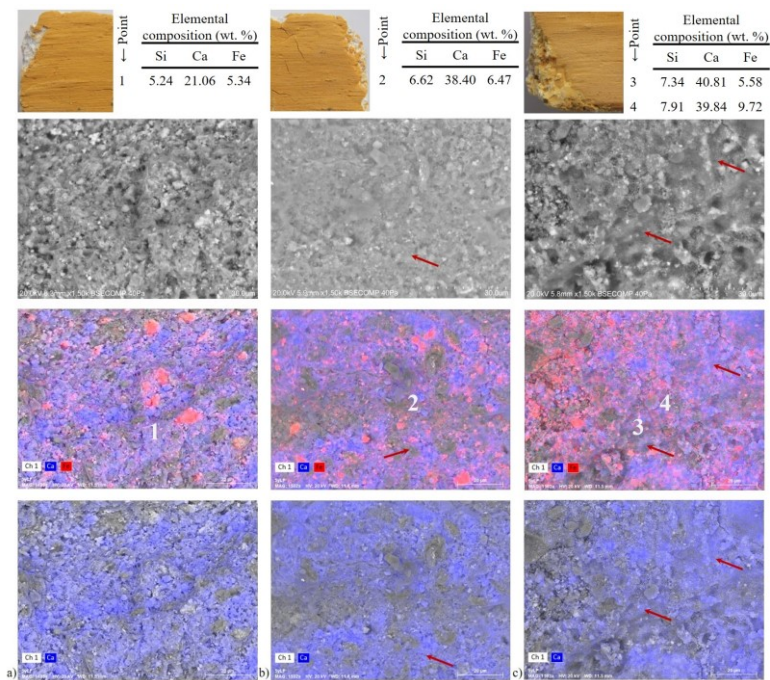


Fig. 6. SEM images (top) and SEM-EDS elemental distribution maps (Ca, Fe – middle; Ca – bottom) of sample y-LF-2. a) Area A - untreated; b) Area B; c) Area D. (Insets: technical photography capture of the analysed area.) Solid line arrows point out the coating layer formed

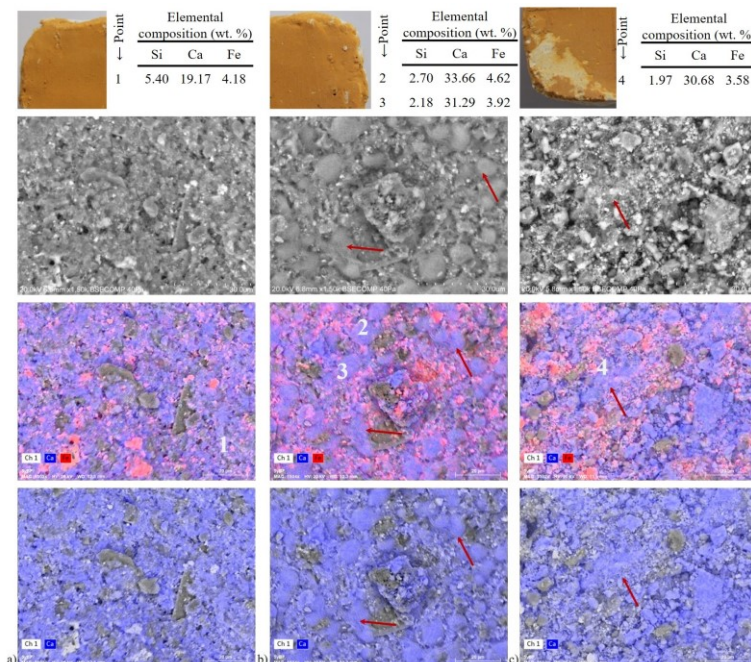


Fig. 7. SEM images (top) and SEM-EDS elemental distribution maps (Ca, Fe – middle; Ca – bottom) of sample y-BF-2. a) Area A - untreated; b) Area B; c) Area D. (Technical photography capture of the analysed area.) Solid line arrows point out the coating layer formed

Actually, even the uncarbonated $\text{Ca}(\text{OH})_2$ nanoparticles may have strengthening capacity [19]. In addition, even though the nanolime particle distribution may be heterogeneous, respectively the converted particles to CaCO_3 polymorphs would also be irregularly distributed, they will still reduce the pores [9], as also suggested by the SEM analysis. The consolidation effectiveness would also depend on the particles' penetration depth and the volatility of the solvent, among other factors. The $\text{Ca}(\text{OH})_2$ particles of the LAB nanolime and the thin coating layers cover pores and spots between the aggregate, calcite matrix, and pigment grains. Thus, they form bridges between aggregate and grains and contribute to the re-cohesion of the paint layers, as is evident from the comparison with the untreated area A. During medium-term ageing, after almost three years, the particles have partially carbonated and have remained in the same place without evidence of detachment from the grains. They appear even more compact due to the coating spot formation, which makes the treatment equally suitable and reliable in the medium term. In any way, both analyses suggest that there is not a significant change in the paint layer or *intonaco* microstructure or morphology besides the partial porosity reduction; therefore, it is not expected that the treatment would significantly affect the physical properties of the replicas.

Overall, the treatments with the two kinds of nanolimes remain effective in terms of re-cohesion of the paint layers and did not cause any surface damage in the medium term (Fig. A1, Appendix A). Some LAB nanolime particles remain spread over the surface as they were one week after treatment; others appear partially carbonated. A further re-cohesion has occurred in three years by forming a thin coating layer. The commercial nanolime also remains reliable in terms of re-cohesion, covering the paint layers with more compact coatings after treatment that have remained without cracks after three years.

The treatments with the commercial acrylic polymer are consistent with what is expected, given that these materials have already been widely used. The thin film formed one week after the treatment in cracks surrounding the pigment grains remains solid three years later (Fig. A1, Appendix A).

The images of all kinds of paint layers treated with the three consolidants (Fig. A1) show that each set of samples has a different texture in the treated areas in comparison to the untreated areas. The chemical composition due to the treatments with nanolime is practically the same or shares some common detectable elements in the case of the commercial acrylic polymer. Although the nanolime concentrations are relatively high (25g/L), the amount of applied material is very low. Consequently, it is expected to be difficult to unambiguously differentiate the newly formed CaCO_3 (or acrylic film) from the original substrate [22], in particular using the EDS analysis. Even though it is possible to distinguish the different surface morphologies of the treated surfaces, given the nanolime's typical shape and smaller dimensions than the substrate grains and the coating-like CaCO_3 appearance. There is an apparent partial re-cohesion that appears in one week and remains undamaged over three years, with no significant visible change in the *intonaco* microstructure or morphology. Therefore, it is not expected that the treatments would significantly affect the morphological properties of the replicas.

Colorimetry and spectrophotometry analysis

The average values of the chromatic coordinate variations determined for all replicas (untreated and treated areas) are shown in Table 2.

Table 2. CIE*L*a*b* coordinates and chromatic variations (average values) using CIE*L*a*b* coordinates calculated for the untreated (U) and treated (T) areas A and B/C of all samples. ΔE^* - total colour variations, ΔL^* , Δa^* , and Δb^* correspond to variations in the colour values in the dark–light, red–green, and yellow–blue axes. Values were calculated according to Equations 1-4 [18] and ΔE^* values meanings and rating scale of incompatibility risk are according to literature [23,24]. (Replicas' designations are summarized in Table 1)

Sample ref.	Area	L*	a*	b*	ΔL^*	Δa^*	Δb^*	ΔE^*_{ab}
b-LF-1	U	62.74±2.79	-0.35±0.26	-17.02±2.48				
	T	66.74±2.78	-0.22±0.30	-17.74±1.22	+3.99	+0.12	-0.72	4.06
Value from the preliminary studies: 1 month after treatment →					(+1.29)	(-0.07)	(+1.29)	(1.8)
<i>Sample is: lighter (+ΔL^*), redder (+Δa^*) and bluer (-Δb^*) than the standard. Medium risk of aesthetic incompatibility ($3 < \Delta E^* < 5$).</i>								
b-LF-2	U	70.50±2.50	-0.59±0.10	-17.90±0.32				
	T	66.58±5.03	-0.42±0.10	-18.19±1.06	-3.92	+0.17	-0.29	3.93
Value from the preliminary studies: 1 month after treatment →					(0.93)	(-0.12)	(0.43)	(1.03)
<i>Sample is: darker (-ΔL^*), redder (+Δa^*) and bluer (-Δb^*) than the standard. Medium risk of aesthetic incompatibility ($3 < \Delta E^* < 5$).</i>								
b-LF-3	U	58.61±6.44	-0.40±0.08	-15.69±1.94				
	T	56.07±4.87	-0.43±0.05	-14.61±1.47	-2.54	-0.03	+1.08	2.76
Value from the preliminary studies: 1 month after treatment →					(1.01)	(-0.02)	(-0.03)	(1.01)
<i>Sample is: darker (-ΔL^*), greener (-Δa^*) and yellow (+Δb^*) than the standard. Low risk of aesthetic incompatibility ($\Delta E^* < 3$).</i>								
y-LF-1	U	71.02±0.48	16.81±0.42	41.41±1.28				
	T	70.07±1.17	15.51±0.44	36.01±1.49	-0.95	-1.30	-5.40	5.64
Value from the preliminary studies: 1 month after treatment →					(1.11)	(-1.25)	(-5.97)	(6.19)
<i>Sample is: darker (-ΔL^*), greener (-Δa^*) and bluer (-Δb^*) than the standard. High risk of aesthetic incompatibility ($\Delta E^* > 5$).</i>								
y-LF-2	U	69.80±2.81	16.64±0.91	42.27±2.36				
	T	70.87±2.22	16.18±0.22	36.64±1.14	+1.07	-0.47	-5.63	5.75
Value from the preliminary studies: 1 month after treatment →					(0.5)	(-0.51)	(-4.37)	(4.39)
<i>Sample is: lighter (+ΔL^*), greener (-Δa^*) and bluer (-Δb^*) than the standard. High risk of aesthetic incompatibility ($\Delta E^* > 5$).</i>								
y-LF-3	U	70.25±3.58	15.99±1.54	40.74±4.58				
	T	70.54±0.73	16.80±0.12	42.32±0.48	+0.29	+0.81	+1.59	1.08
Value from the preliminary studies: 1 month after treatment →					(-1.07)	(0.06)	(-0.71)	(1.28)
<i>Sample is: lighter (+ΔL^*), redder (+Δa^*) and yellow (Δb^*) than the standard. Low risk of aesthetic incompatibility ($\Delta E^* < 3$).</i>								
y-BF-1	U	64.67±0.60	18.54±0.60	42.25±1.12				
	T	68.61±0.94	18.83±0.48	39.85±1.64	+3.95	+0.29	-2.39	4.62
Value from the preliminary studies: 1 month after treatment →					(1.2)	(-0.57)	(-5.76)	(5.91)
<i>Sample is: lighter (+ΔL^*), redder (+Δa^*) and yellow (-Δb^*) than the standard. Medium risk of aesthetic incompatibility ($3 < \Delta E^* < 5$).</i>								
y-BF-2	U	63.49±0.82	18.09±0.14	42.70±0.22				
	T	66.15±2.64	18.12±0.88	36.80±2.93	+2.66	+0.02	-5.90	6.48
Value from the preliminary studies: 1 month after treatment →					(0.35)	(0.25)	(-4.45)	(4.47)
<i>Sample is: lighter (+ΔL^*), redder (+Δa^*) and bluer (-Δb^*) than the standard. High risk of aesthetic incompatibility ($\Delta E^* > 5$).</i>								
y-BF-3	U	67.03±1.58	20.85±1.59	45.52±1.97				
	T	68.54±1.30	20.61±1.11	45.31±1.72	+1.51	-0.24	-0.21	1.54
Value from the preliminary studies: 1 month after treatment →					(-0.14)	(-0.26)	(-0.97)	(1.01)
<i>Sample is: lighter (+ΔL^*), greener (-Δa^*) and bluer (-Δb^*) than the standard. Low risk of aesthetic incompatibility ($\Delta E^* < 3$).</i>								

The presence of a white haze on the paint layers already found in our preliminary results was ascertained by spectrophotometry and colorimetry analysis (Fig. 8). No change in the shape of the reflectance spectral curves was detected in both painting techniques (LF and BF) in the pigments used, suggesting that the pigments did not suffer significant physicochemical alteration in the middle term.

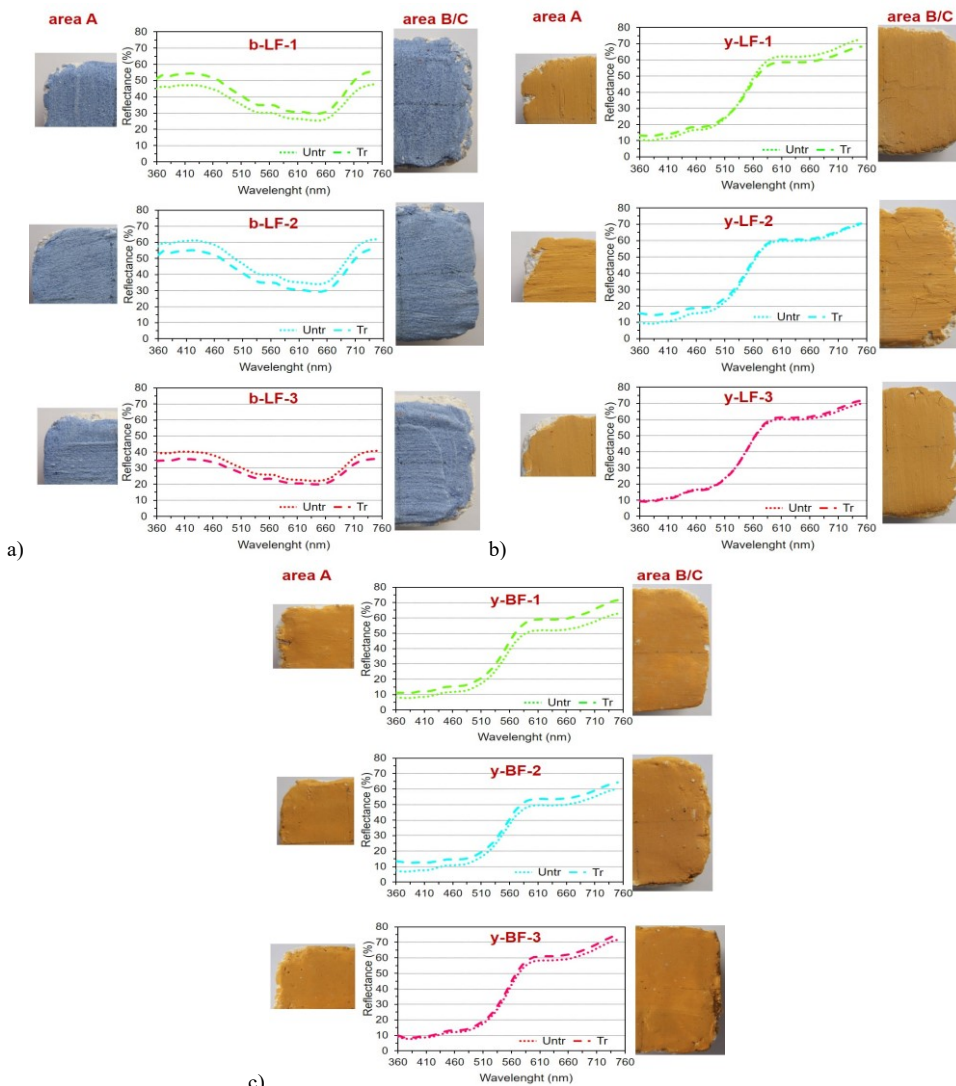


Fig. 8. Visible technical photography documentation and reflectance spectral curves of paint layers consolidated with the three consolidants:

a) Samples bLF; b) Samples yLF; c) Samples yBF. *Area A* - untreated, *area B/C* - treated; both of natural lack of cohesion

By comparing the paint layers documented photographically (Fig. 1a and insets in Fig. 8), in particular, both untreated (A) and treated areas (B/C), the white haze on the blue paint layers and the yellow paint layers treated with the acrylic resin is not noticeable to the naked eye. It is somehow possible to observe a white haze in the form of some translucent whitish spots over the treated paint layer of replica y-BF-1 (LAB nanolime), similar to the spots already observed one week after treatment [15]. The treated areas (B/C) of replicas y-LF-1 (LAB

nanolime), y-LF-2, and y-BF-2 (commercial nanolime) seem to be visually slightly lighter in comparison to reference area A.

The small layers have remained uninduced by the treatments' changes in the visual colour perception since the preliminary analyses. We have already assigned this behaviour to the low hiding power of small, coarse particles in a white calcium matrix [15]. Although increased, the ΔE^*_{ab} values - 4.06 (b-LF-1), 3.93 (b-LF-2), and 2.76 (b-LF-3) - are in the range of low to medium risk of aesthetic incompatibility (Table 2) [23, 24]. For several cases reported in the literature, ΔE^* values could be assumed to be slight for consolidants when below 5 and not highly relevant to the naked eye, while values above 5 indicate colour changes visible to the naked eye [23, 25]. The ochre paint layers treated with Primal[®] also remain unchanged after the treatment, which is consistent with the very diluted and small amount of consolidant that was applied (2% in tap water). The lack of observable aesthetical change in this case is also confirmed by the SEM analyses, where the film scarcely covers some pores, and this is consistent with the ΔE^*_{ab} values 1.08 (y-LF-3) and 1.54 (y-BF-3), both indicating a low risk of aesthetic incompatibility.

The appearance of the whitish spots that were detected visually for samples y-BF-1 is illustrated in the reflectance spectral curves of the untreated and treated areas of this replica (Fig. 8c). The reflectance (R%), although increasing only slightly, shows the biggest increase compared to the spectral curves of the other replicas. The SEM analysis of this replica has shown a more compact particle distribution. Yet the treatment has caused only a medium risk of aesthetic incompatibility (ΔE^*_{ab} 4.62), where the value of ΔE^*_{ab} has decreased for the three years of ageing from 5.91. The denser, spherical-like spots observed over the paint layer of y-BF-2 caused the highest value of ΔE^*_{ab} , 6.48, indicating a high risk of aesthetic incompatibility. The values of yellowness (b^*) of treated with nanolime areas of all layers of y-BF are lower than the values for the untreated area (Table 2) (also consistent with these values for yellow replicas that decreased immediately after treatment with LAB nanolime), while their lightness increases; b^* and L^* of y-BF-3 are nearly the same.

The values of yellowness (b^*) of treated areas of replicas y-LF are lower than the values found for the untreated area, which is coherent with these values for yellow replicas that decreased immediately after treatment with LAB nanolime. The L^* and a^* values are very close (the spectral curves of untreated and treated areas almost overlap). However, ΔE^*_{ab} suggests a high risk of aesthetic incompatibility with very close values caused by both nanolimes: 5.64 (y-LF-1) and 5.75 (y-LF-2) [23-25], explained by the large number of nanoparticle clusters after the LAB nanolime treatment (y-LF-1) and the compact coating after commercial nanolime treatment (Fig. 8b).

In terms of risk of aesthetic incompatibility, the treatments were most favourable for paint layers with small pigment, while the treatments of ochre paint layers were on average near high risk, probably due to the high concentrations of the applied nanolimes (25g/L).

The nanolime consolidants that lead to the formation of a coating layer and/or tend to form clustered particles induce higher colour changes than Primal[®], in agreement with other reports [9, 26]. The ΔE^*_{ab} values of the yellow layers are also expected given the increased hiding power of the ochre pigment. The values show that as the morphology remains constant over time, the chromatic variations, in general, remain relatively constant, except for a few ΔE^*_{ab} that have increased over time, but not significantly. Although the ΔE^*_{ab} values are lower for the small pigment, there is not a significant variation in this value with the pigment or painting technique applied. Further studies with lower consolidant concentrations could provide useful information on the possible control of the possible white veil formation; such assays could take place at months intervals after the treatment in order to follow the coating formation in the case of the LAB nanolime.

Conclusions

This paper demonstrates that laboratory-prepared nanolime, as the commercial products, maintains its effect on the paint layer morphology over a longer time interval. Consequently, it has a strong potential to be efficient in the medium term. Any possible aesthetical changes occur immediately after the treatment and maintain a relatively constant value over time. The LAB nanoparticles are spread over the surface in clusters, uncarbonated and partially

carbonated, and there are thin coatings that have been formed over the three years of ageing. These coatings are similar, but less compact, compared to the commercial nanolime particles. The former coatings have remained unchanged upon ageing during the next three years, maintaining the re-cohesion of the paint layer and making them as efficient as immediately after the treatment, given that no detachments or cracks are present.

Despite the favourable results, further studies under different ageing conditions, nanolime concentrations, and solvents associated with pigment nature and preparation techniques should be performed *in vitro*. For conservation studies, these consolidants should be applied in concentrations lower than 25g/L, and relative humidity and temperature should also be carefully considered before an intervention. Assessment of the mechanical resistance of replicas treated with the best formulation could also be considered.

Acknowledgments

The authors acknowledge Fundação para a Ciência e a Tecnologia (Portugal) for the funding support through projects PTDC/ART-HIS/1370/2020-Unveiling the mural painting Art of Almada Negreiros (1938-1956), UIDB/04449/2020 and UIDP/04449/2020 and contract programs of Ref. DL 57/2016/CP1372/CT0013 (PG), DL/57/2016/CP1338/CT0001 and and Ref.^a CEECINST/00069/2021 (MG).

References

- [1] * * *, **ICOMOS Principles for the preservation and conservation/restoration of wall paintings. Ratified by the ICOMOS 14th General Assembly**, in Victoria Falls, Zimbabwe, Oct 2003. URL: <https://www.icomos.org/en/what-we-do/focus/179-articles-en-francais/ressources/charters-and-standards/166-icomosprinciples-for-the-preservation-and-conservationrestoration-of-wall-paintings> [accessed on July/Aug 2023].
- [2] D. Chelazzi, P. Baglioni, *From Nanoparticles to Gels: A Breakthrough in Art Conservation Science*, **Langmuir**, **39**(31), 2023, pp. 10744-10755.
- [3] C. Rodriguez-Navarro, E. Ruiz-Agudo, *Nanolimes: from synthesis to application*, **Pure and Applied Chemistry**, **90**, 2018, pp. 523-550.
- [4] P.I. Girginova, C. Galacho, R. Veiga, A. Santos Silva, A. Candeias, *Inorganic Nanomaterials for Restoration of Cultural Heritage: Synthesis Approaches towards Nanoconsolidants for Stone and Wall Paintings*, **ChemSusChem**, **11**, 2018, pp. 4168-4182.
- [5] J. Zhu, P. Zhang, J. Ding, Y. Dong, Y. Cao, W. Dong, X. Zhao, X. Li, M. Camaiti, *Nano Ca(OH)₂: A review on synthesis, properties and applications*, **Journal of Cultural Heritage**, **50**, 2021, pp. 25-42.
- [6] M. Ambrosi, L. Dei, L., R. Giorgi, C. Neto, P. Baglioni, *Colloidal Particles of Ca(OH)₂: Properties and Applications to Restoration of Frescoes*, **Langmuir**, **17**, 2018, pp. 4251-4255.
- [7] G. Borsoi, B. Lubelli, R. van Hees, R. Veiga, A.S. Silva, L. Colla, L. Fedele, P. Tomasin, *Effect of solvent on nanolime transport within limestone: How to improve in-depth deposition*, **Colloids and Surfaces A: Physicochemical and Engineering Aspects**, **497**, 2016, pp. 171-181.
- [8] J.S. Pozo-Antonio, J. Otero, *The influence of using wet cellulose poultice on nanolime consolidation treatments applied on a limestone*, **Construction and Building Materials**, **337**, 2022, Article number: 127615.
- [9] C. Serrano Aranda, M.A. Zalbidea Munoz, M. Bea Martinez, *Selection of consolidating products. Tests and studies for the cohesion of the support of Los Toros del Prado del Navazo shelter (Albarracin, Teruel)*, **Ge-Conservacion**, **22**(1), 2022, pp. 76-89.
- [10] T. López-Martínez, J. Otero, J., *Preventing the Undesired Surface Veiling after Nanolime Treatments on Wall Paintings: Preliminary Investigations*, **Coatings**, **11**, 2021, Article number: 1083.
- [11] L. Normand, S. Duchêne, V. Vergès-Belmin, C. Dandrel, D. Giovannacci, W. Nowik, *Comparative in Situ Study of Nanolime, Ethyl Silicate and Acrylic Resin for Consolidation of Wall Paintings with High Water and Salt Contents at the Chapter Hall of Chartres Cathedral*, **International Journal of Architectural Heritage**, **14**, 2020, pp. 1120-1133.

- [12] M. Gil, T. Rosado, I. Ribeiro, J.A. Pestana, A.T. Caldeira, M.L. Carvalho, L. Dias, J. Mirão, A. Candeias, *Are they fresco paintings? Technical and material study of Casas Pintadas of Vasco da Gama house in Évora (Southern Portugal)*, **X-Ray Spectrometry**, **44**, 2015, pp. 154-162.
- [13] P.I. Girginova, C. Galacho, R. Veiga, A. Santos Silva, A. Candeias, *Study of mechanical properties of alkaline earth hydroxide nanoconsolidants for lime mortars*, **Construction and Building Materials**, **236**, 2020, Article number: 117520.
- [14] M. Gil, *Lime paintings in treatises and construction technical manuals in Portugal from 1880 to 1931 - an historical review*, **Conservar Património**, **39**, 2022, pp. 45-60.
- [15] B. Baiza, M. Gil, C. Galacho, A. Candeias, P. I. Girginova, *Preliminary Studies of the Effects of Nanoconsolidants on Mural Paint Layers with a Lack of Cohesion*, **Heritage**, **4**, 2021, pp. 3288-3306.
- [16] M. Gil, M.L. Carvalho, S. Longelin, I. Ribeiro, S. Valadas, J. Mirão, A. E. Candeias, *Blue Pigment Colors from Wall Painting Churches in Danger (Portugal 15th to 18th Century): Identification, Diagnosis, and Color Evaluation*, **Applied Spectroscopy**, **65**, 2011, pp. 782-789.
- [17] A. Coccato, L. Moens, P. Vandenaabeele, *On the stability of mediaeval inorganic pigments: a literature review of the effect of climate, material selection, biological activity, analysis and conservation treatments*, **Heritage Science**, **5**, 2017, Article number: 12.
- [18] R. Johnston-Feller, **Color Science in the Examination of Museum Objects: Nondestructive Procedures. Tools for conservation**, Los Angeles, CA: Getty Conservation Institute, 2001.
- [19] J. Otero, A. E. Charola, V. Starinieri, "Preliminary Investigations of Compatible Nanolime Treatments on Indiana Limestone and Weathered Marble Stone", **International Journal of Architectural Heritage**, **16**, 2022, pp. 394-404.
- [20] A. Michalopoulou, P.N. Maravelaki, V. Kilikoglou, I. Karatasios, *Morphological characterization of water-based nanolime dispersions*, **Journal of Cultural Heritage**, **46**, 2020, pp. 11-20.
- [21] R. Camerini, G. Poggi, D. Chelazzi, F. Ridi, R. Giorgi, P. Baglioni, *The carbonation kinetics of calcium hydroxide nanoparticles: A Boundary Nucleation and Growth description*, **Journal of Colloid and Interface Science**, **547**, 2019, pp. 370-381.
- [22] J. Vojtechovsky, *Surface consolidation of wall paintings using lime nano-suspensions*, **Acta Polytechnica**, **57**, 2017, pp. 139-148.
- [23] J. Delgado Rodrigues, A. Grossi, *Indicators and ratings for the compatibility assessment of conservation actions*, **Journal of Cultural Heritage**, **8**(1), 2007, pp. 32-43.
- [24] A. Pondelak, S. Kramar, M. L. Kikelj, A. S. Škapin, *In-situ study of the consolidation of wall paintings using commercial and newly developed consolidants*, **Journal of Cultural Heritage**, **28**, pp. 1-8.
- [25] B. Sena da Fonseca, A. P. Ferreira Pinto, S. Piçarra, M. F. Montemor, *The potential action of single functionalization treatments and combined treatments for the consolidation of carbonate stones*, **Construction and Building Materials**, **163**, 2018, pp. 586-599.
- [26] E. Bourguignon, P. Tomasin, V. Detalle, J.-M. Vallet, M. Labouré, I. Olteanu, M. Favaro, M. A. Chiurato, A. Bernardi, F. Becherini, *Calcium alkoxides as alternative consolidants for wall paintings: Evaluation of their performance in laboratory and on site, on model and original samples, in comparison to conventional products*, **Journal of Cultural Heritage**, **29**, 2018, pp. 54-66.

Received: February 05, 2023

Accepted: August 18, 2023

Appendix A. Electron microscopy analysis

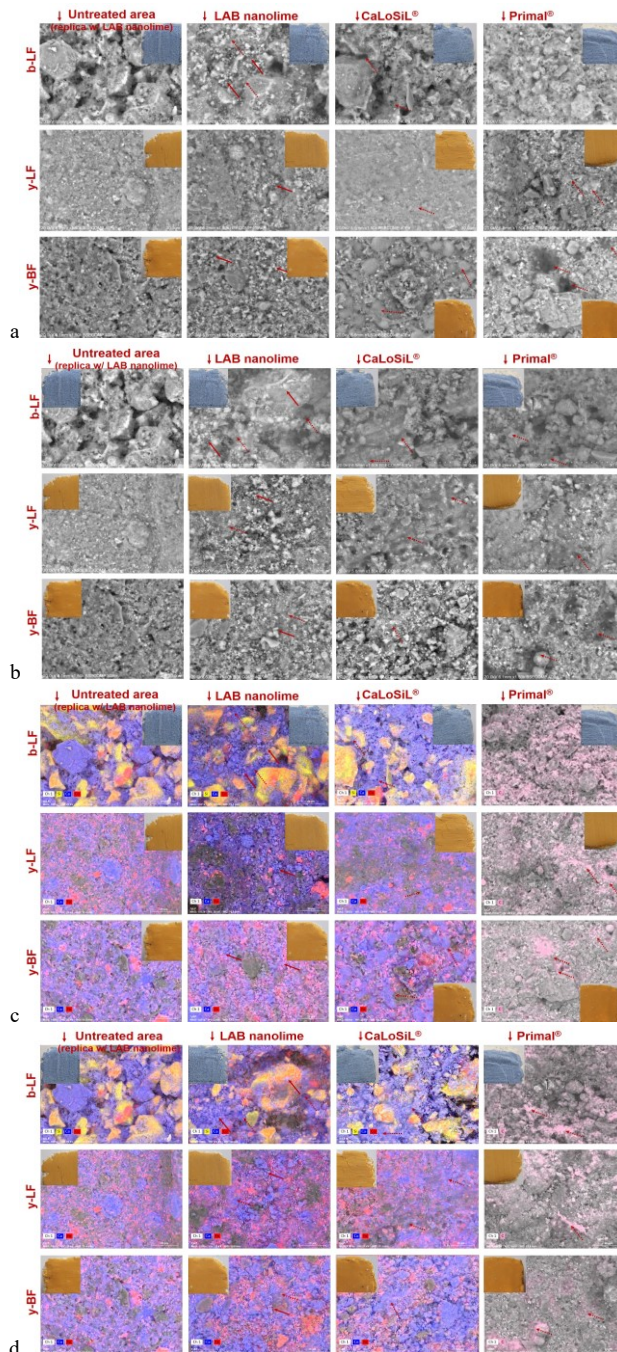


Fig. A1. SEM images and SEM-EDS elemental maps (Ca, Co (small samples); Ca, Fe (ochre samples); C (samples treated with Primal®)): a comparison between all samples: a) Areas B/C compared to area A; b) Areas D compared to area A; c) Elemental map of areas B/C compared to area A; d) Elemental map of areas D compared to area A. (Solid line arrows point out the coating layer formations)